

Corticothalamic projections control synchronization in locally coupled bistable thalamic oscillators

Jörg Mayer¹, Heinz Georg Schuster¹, Jens Christian Claussen¹, Matthias Mölle²

¹*Institute for Theoretical Physics and Astrophysics, University of Kiel, 24098 Kiel, Germany*

²*Department of Neuroendocrinology, University of Lübeck, 23538 Lübeck, Germany*

(Dated: February 7, 2007. Accepted July 5, 2007)

Thalamic circuits are able to generate state-dependent oscillations of different frequencies and degrees of synchronization. However, little is known how synchronous oscillations, like spindle oscillations in the thalamus, are organized in the intact brain. Experimental findings suggest that the simultaneous occurrence of spindle oscillations over widespread territories of the thalamus is due to the corticothalamic projections, as the synchrony is lost in the decorticated thalamus. In this Letter we study the influence of corticothalamic projections on the synchrony in a thalamic network, and uncover the underlying control mechanism, leading to a control method which is applicable for several types of oscillations in the central nervous system.

PACS numbers: 87.19.La 05.45.-a 87.19.Nn 84.35.+i

Coupled oscillators are abundant in physics [1, 2], chemistry [3] and biology [4–6]. Whenever large numbers of coupled oscillators are considered, the collective behavior of the ensemble is of great interest [2, 7]. A widespread phenomenon in populations of periodic, noisy and chaotic oscillators (or maps) is the appearance of synchronous collective oscillations, studied theoretically [7] as well as experimentally [3, 8]. In neural systems the phenomenon of spike burst activity is widespread and of great importance [9, 10]. This activity is characterized by a recurrent transition between a resting state and a firing state with a burst of multiple spikes. Bursting is a multiple time scale effect and appears due to a slow process which modulates a fast subsystem [9, 11].

Neural cells in the thalamus are known to exhibit spike burst activity during periods of drowsiness, inattentiveness and sleep [12, 13]. Spindle oscillations, a hallmark of early sleep stages, observed in the electroencephalographic recordings of sleeping humans as oscillations in a 12-15 Hz frequency range, are considered to be the result of synchronized spike burst activity of millions of neurons in the thalamus [10, 15]. Despite experimental findings in thalamic slices, where the spindle oscillations propagate like a traveling wave through the network [14], in the intact brain spindle oscillations occur almost synchronously over widespread territories of the thalamus [15, 16]. These contrasting results between in vitro and in vivo experiments occur due to the absence of corticothalamic projections (synaptic connections from the cortex to the thalamus) in a thalamic slice as, after ablation of the cortex, synchrony is lost in the thalamus [15–17].

In a coupled system of oscillators, oscillations become more and more coherent when the coupling strength is increased [2, 7]. In this Letter, we explore the possibility to induce the transition from the decoherent state to the coherent state – in which bursts occur synchronously – by external signals. For this reason, we investigate the mechanism by

which corticothalamic projections control coherence of thalamic spindle oscillations. The knowledge of control mechanisms for synchrony in neural systems may help to understand the origins and mechanisms of sleep and other processes in the mammalian brain, and – in the long run – to control them.

The Letter is organized as follows: We introduce our simplified model of the thalamocortical oscillator based on [13, 18]. Then we study burst-synchronization quasi-analytically for two coupled neurons. Finally, we study the collective behavior of thalamic oscillators, verify the experimental observation that corticothalamic projections control synchrony in the thalamus by using human slow wave EEG data to control our computational thalamus model.

The dynamics of the system described in [18] is mainly determined by a slow change between a bistable state where a stable fixed point and a stable limit cycle coexist, and a monostable state where only a stable fixed point exists. This behavior can be described by a slowly modulated overdamped movement of a particle in a rotating symmetric time-dependent double well potential

$$U(r, t, \varphi) = \frac{1}{2}r^2 - \frac{1}{4}\alpha(t)r^4 + \frac{1}{6}r^6 \quad (1)$$

(see Fig. 1), where $r = \sqrt{x^2 + y^2}$, and $\varphi(t) = \omega t$ captures the oscillation in phase (mod 2π), see Ref. [19] for a related model. Depending on the slow variable $\alpha(t)$, the system possesses either one stable fixed point, or it shows bistability with a stable fixed point and a stable limit-cycle. As the relaxation within the wells is fast compared to $\alpha(t)$, so the quasi-adiabatic approximation is applicable. We get an equation for the movement in r direction for the single oscillator:

$$\begin{aligned} \dot{r} &= -\partial U(r, \alpha)/\partial r + I^{\text{ext}} + F(t) \\ \dot{u} &= \mu(r(1-u) - 0.375u), \end{aligned} \quad (2)$$

where $\alpha(t) = a(1-u)$, $F(t)$ is a common control signal.

Following [9], we first study synchrony in two bistable elements coupled linearly via r :

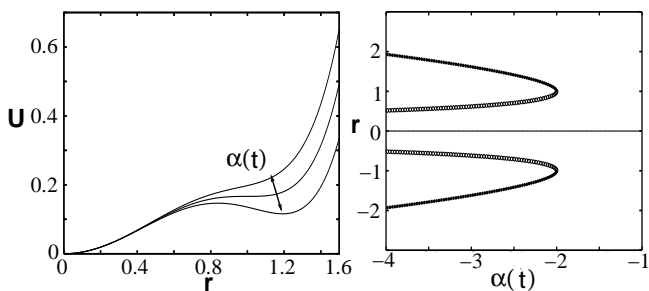


FIG. 1: Depending on α , the system possesses either one stable fixed point or it shows bistability with a stable fixed point and a stable limit-cycle. Left: $U(r, t, \varphi)$ for different values of α . Right: Bifurcation diagram of (2) with $\alpha(t)$ considered as a bifurcation parameter. Solid lines indicate a stable fixed point, open circles an unstable limit cycle and filled circles a stable limit cycle.

$$\begin{aligned} \dot{r}_i &= -r_i + a(1 - u_i)r_i^3 - r_i^5 + I_i^{\text{ext}} + \epsilon r_j \\ \dot{u}_i &= \mu(r_i(1 - u_i) - 0.375u_i), \end{aligned} \quad (3)$$

where $\epsilon > 0$ is the coupling strength, $\mu = 0.0004$ scales the refractory period $\tau \sim \mu^{-1}$ and $a = 2.5$ is chosen such that $U(r, \alpha)$ is a double well potential for $u < 0.2$, and $i \neq j$ respectively are the indices. I_i^{ext} is the external input, which is a Poisson distributed shotnoise with a rate of 1/100ms, refractory period of 30ms, pulse duration of 2ms and an amplitude of 0.6. We emphasize that the I_i^{ext} are stochastically independent, so $\langle I_i^{\text{ext}}, I_j^{\text{ext}} \rangle = \delta_{i,j}$. Through the coupling the potentials of the bistable elements get deformed

$$U_i(r_i, \alpha_i, \epsilon) = \frac{1}{2}r_i^2 - \frac{1}{4}\alpha_i(t)r_i^4 + \frac{1}{6}r_i^6 - \epsilon r_j r_i, \quad (4)$$

where $i \neq j$ respectively are the indices. If neuron 2 has just become excited, i.e. it stays in the right well in Fig. 1, then $u_2 \simeq 0.15$ and $r_2 \simeq 1.25$. Further we assume that neuron 1 is in the ground state and does not get an input spike. Mutual synchronization will occur if $U_1(r_i, \alpha_i, \epsilon)$ gets so strongly deformed that the barrier between the two wells vanishes, i.e. only the external well persists. This is the case if $\partial U / \partial r = 0$ is fulfilled in only one point for $r \in (0, \infty)$. The transition point can be calculated by applying Sturm's theorem [20], accordingly synchronization of inter-well jumps should occur at $\epsilon \simeq 0.23$. The estimation above only gives the values of ϵ where r synchronizes, but however as u obeys a linear differential equation, which gets activated by r , we expect u to synchronize at the same value of ϵ as r . The numerical simulation of (3) for different ϵ in Fig. 2 verifies this argumentation.

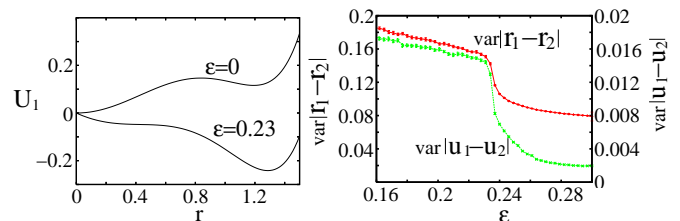


FIG. 2: (color online) left: The potential U_1 with no coupling and $u = 0.15$ and for the case that neuron 2 is in the excited state and $u_{1/2}$ are both 0.15 for a coupling strength of $\epsilon = 0.23$. see (4) and Fig. 1. right: Variations of $|r_1 - r_2|$ (red) and $|u_1 - u_2|$ (green/light grey) as a function of ϵ . As the inter-well jumps synchronize at $\epsilon \simeq 0.23$, the variations of $|r_1 - r_2|$ and $|u_1 - u_2|$ rapidly decrease at this point.

Our goal is to induce the transition to synchrony by external control signals. Having clinical applications in mind, desiring to achieve large effects with weak external triggers, we want the external control signal to support the internal dynamics of the coupled system, i.e. both the open loop control signal and the internal coupling will be needed to induce the transition to synchrony. At this point we present a qualitative understanding of a control mechanism which is based on the dynamics of the reciprocal coupled oscillators presented above, but is also applicable in larger networks. We assume the slow process $u_i(t)$ to be a relaxation oscillator with relaxation time τ , which scales with μ^{-1} , this relaxation process gets activated by the variable $r_i(t)$, in turn $u_i(t)$ inhibits excitation of r_i during the relaxation time τ . So $u_i(t)$ can be interpreted as a refractory process which leads to a dead time, in which the single oscillator is not excitable. So the maximum phase difference between any arbitrary chosen oscillators is at most of the magnitude of τ . Another way to block excitation of the r_i is a common, sufficiently strong hyperpolarization (i.e. $F(t)$ is negative) of all oscillators. If the duration of this hyperpolarization exceeds τ , the $u_i(t)$ will decay back to the excitable ground state. That means they all have the same phase. Of course the phase of the $u_i(t)$ can diffuse in time because of the highly stochastic input. But if the phase resetting is done repetitively, the variance of the phases of u_i can be confined. The amplitude of the hyperpolarization depends on the amplitude of the Poisson distributed input spikes, it has to be strong enough to suppress excitation of the r_i . Numerically we find $\tau \approx 4.96$ s and the system stays in the excited state for $T_e = 0.45$ s. Just like the coupling, also an external control signal deforms the potential, and, if applied appropriately, interacts in a promotive way for synchronization with the intrinsic dynamics of the coupled oscillators. We choose

$F(t)$ to be a periodic train of square pulses with a pulse height $F = 0.1$ and pulse duration T_e . The positive part of $F(t)$ results in an amplification of the coupling strength ϵ . Between the pulses there is an inactive phase where $F = -0.1$ lasting τ s (see Fig. 3),

$$U(r_i, \alpha_i, \epsilon)_i = \frac{1}{2}r_i^2 - \frac{1}{4}\alpha_i(t)r_i^4 + \frac{1}{6}r_i^6 - (\epsilon r_j + F(t))r_i. \quad (5)$$

If we further assume that the u_i have been reset to their groundstate by the negative part of the control signal, the first well vanishes at $\epsilon \simeq 0.14$ resulting in synchronization of inter-well jumps. The simulation of (5) for different ϵ in Fig. 3 verifies this argumentation. In the remainder, we will use cortical slow wave EEG data as the control signal. Taken together, this common signal combined with an internal nearest neighbor coupling, should lead to synchronous network oscillations.

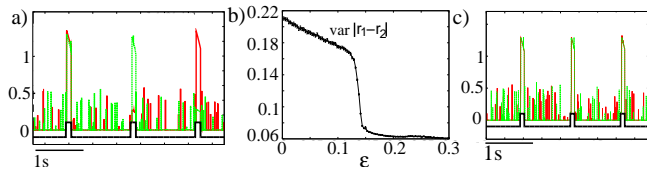


FIG. 3: (color online) a) and c) : r_1 (red), r_2 (green/light grey) and $F(t)$. a): For a coupling strength of $\epsilon = 0.12$ the inter-well jumps occur asynchronously. b): Variations of $|r_1 - r_2|$ as a function of ϵ , both oscillators were modulated by $F(t)$. As the inter-well jumps synchronize at $\epsilon \simeq 0.14$, the variations of $|r_1 - r_2|$ rapidly decrease. For the parameters chosen here, both control signal and internal coupling are needed. c): For $\epsilon = 0.15$ the inter-well jumps occur synchronously, triggered by $F(t)$.

Now we model the thalamic network by a 2-dimensional 50×50 square lattice,

$$\begin{pmatrix} \dot{r}_{ij} \\ \dot{u}_{ij} \end{pmatrix} = \vec{F}(r_{ij}, u_{ij}) + \epsilon \begin{pmatrix} \sum_{i'j'} G_{ij i'j'} r_{i'j'} \\ 0 \end{pmatrix} + F^{\text{ext}}(t) \quad (6)$$

where the uncoupled dynamics of the i -th node obeys $\vec{F}(r_{ij}, u_{ij})$ given by (2) and G determines the coupling between the neurons. $F^{\text{ext}}(t) = \kappa \mathcal{E}(t)$ is the common external forcing which consists of human slow wave sleep EEG-data $\mathcal{E}(t)$. Almost any coupling scheme can be cast into the form of (6) by choosing the right G matrix [23], here we use a linear nearest neighbor coupling with radius 1 without self-loops. In a first instance, we study the system without external control, such $F(t) = 0$. Depending on ϵ , we observe four different kinds of collective phenomena. For $\epsilon < 0.029$ the oscillators are desynchronized. Due to the nearest neighbor coupling for $0.029 < \epsilon < 0.057$ bursts propagate like traveling waves through the network. For $\epsilon > 0.057$, burst-synchronization occurs (see Fig. 4). For even larger ϵ , a trivial homogeneous

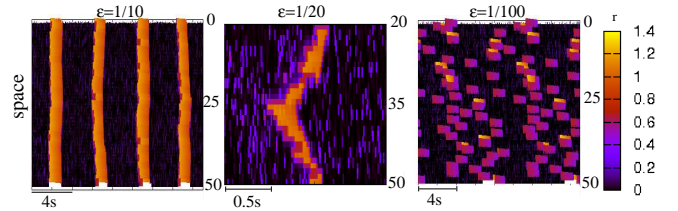


FIG. 4: (color online) Depending on ϵ the network shows either asynchronous ($\epsilon < 0.029$) or synchronous oscillations ($\epsilon > 0.057$). Between these two states traveling waves occur.

state (not shown) occurs. Now we use the meanfield activity as a measure for the degree of synchrony in the system [2]. Here we are mainly interested in the transition of the traveling bursts to synchronous network bursts, and the possibility to induce this transition by an external control signal. As mentioned above, it was observed in thalamic slices that spindle oscillations propagate in a way similar to traveling waves in the absence of corticothalamic projections [15, 16]. In [10] it was examined whether a comparable temporal grouping of spindle activity, coinciding with cortical slow wave oscillations can be found during human slow wave sleep. The results clearly show that also in the human sleep the spindles become synchronized by corticothalamic projections. This phenomenon was part of several numerical and experimental investigations [17, 24] however, the dynamical mechanisms how cortical slow waves lead to coherent spikes in the thalamus are still unknown.

Finally, we verify our approach computationally in comparison with experimental data. Consequently, we use a hybrid network consisting of a computational model of the thalamic slice, which gets real slow wave sleep EEG-data as a common input, to investigate the control of coherence in the thalamic network. While one might argue that the architecture of this model does not reflect nature in detail, as the thalamocortical projections are completely neglected, one reason for this approximation is the fact that the corticothalamic projections outnumber the thalamocortical projections by an order of magnitude [15]; second it was shown that slow waves also occur with extensive destruction of the thalamus and transected corpus callosum; these facts indicate that the thalamus is not essentially involved in the genesis of slow wave rhythm [6]. From both reasons and the results shown in Fig 5 a) and b) we post that synchronization in the thalamus mainly is controlled through open loop repetitive phase resetting by the cortex, in the same way as described above for the two neuron network. The results obtained by our hybrid network (see Fig 5) provide a minimal model comparable with the experimental results in [10].

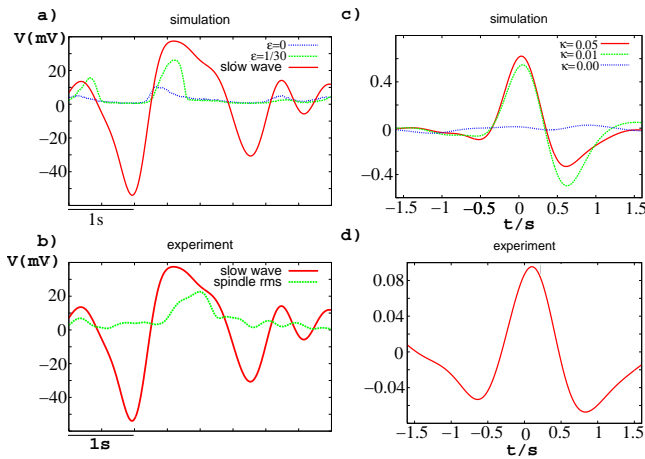


FIG. 5: (color online) Correlation of meanfield network activity $V = \frac{1}{2500} \sum_i^{50} \sum_j^{50} r_{ij}$ with driving input signal depending on the driving parameter κ for $\epsilon = 1/30$. a) and b): Numerical simulation of the network driven by the same EEG spindle sleep data as measured in the experiment[10]. For $\kappa = 0.0$ correlations vanish. a) shows that the internal coupling is needed for proper synchronization as without it the meanfield only shows little variations, the reason for this effect is the same as described above for the two neuron network. c) and d): The corresponding experimentally obtained correlations between spindle rms which corresponds to the r_{ij} scaled by a factor of 30 and EEG activity.

The effect described above was modeled by Steriades group based on conductance based neuron models [26]. In this detailed biophysical neuron models the dead time or refractory period between two spindle oscillations is caused by the I_h [13] current, which corresponds to the slow variable u in our model. In both systems, coherence of thalamic spindles is established by a reset of the slow refractory variable. Our reduced model now allows to identify the dynamical mechanism of this control process by means of threshold modulation. Further, the synchronizing effect gets increased by the depolarizing part of the control signal. As the key mechanism is the reset of the slow refractory variable, this control mechanism should be applicable for a wide range of bistable systems with a slow refractory variable, as cortical slow waves and other neural systems.

To conclude, we have studied the synchronizing influence of corticothalamic projections in a thalamic network by a theoretical model and computationally reproduced the experiment. As the model equations (apart from parameter choices) do not rely specifically on a neural substrate, we anticipate the qualitative behavior to be generic also for other stochastically driven systems composed of excitable units, like several types of oscillations in the central nervous system.

This research has been supported by the Deutsche Forschungsgemeinschaft (SFB 654 ‘‘Plasticity and Sleep’’). We thank Jan Born and Lisa Marshall for intensive and fruitful discussions.

-
- [1] K. Wiesenfeld, J. W. Swift, Phys. Rev. E **51**, 1020 (1994), K. Wiesenfeld, C. Bracikowski, G. James, R. Roy, Phys. Rev. Lett **65**, 1749 (1990)
 - [2] M. G. Rosenblum, A. S. Pikovsky, Phys. Rev. Lett **92**, 114102 (2004)
 - [3] I.Z. Kiss, Y. Zhai, and J.L. Hudson, Phys. Rev. Lett **88**, 238301 (2002); Science **296**, 1676 (2002)
 - [4] J. Buck, E. Buck, Science **159**, 1319 (1968)
 - [5] T. J. Walker, Science **166**, 891 (1969)
 - [6] M. Steriade, A. Nuñez, F. Amzica, Journal of Neuroscience, **13**, 3266, (1993)
 - [7] Y. Kuramoto, Chemical Oscillations, Waves & Turbulence, Springer (1984); Physica D **50**, 15 (1990); A.S. Pikovsky, M.G. Rosenblum, J. Kurths, EPL **34**, 165 (1996), N.F. Rulkov, PRL **86**, 183 (2001)
 - [8] Z. Neda, E. Ravasz, Y. Brechet, T. Vicsek, A. L. Barabasi, Nature, London, **403**, 849 (2000)
 - [9] M. Dhamala, V. K. Jirsa, M. Ding, Phys. Rev. Lett **92**, 28101 (2004)
 - [10] M. Mölle, L. Marshall, S. Gais and J. Born, Journal of Neuroscience, **22**, 10941, (2002)
 - [11] J.L. Hindmarsh, R.M. Rose, Proc. R. Soc. Lond. B **221**, 87 (1984)
 - [12] M. Steriade, The Intact and Sliced Brain, MIT Press (2001)
 - [13] A. Destexhe, A. Babloyantz, T. J. Sejnowski, Biophysical Journal **65**, 1538, (1993)
 - [14] U. Kim, M. V. Sanchez-Vives, D. A. McCormick, Science, **278**, 130, (2000)
 - [15] M. Steriade, PNAS, **98**, 3625 (2001)
 - [16] A. Destexhe, J. Physiol. (Paris) **94**, 391, (2000)
 - [17] D. Contreras, A. Destexhe, T. J. Sejnowski, M. Steriade, Science, **274**, 771, (1996)
 - [18] J. Mayer, H. G. Schuster, J. C. Claussen, Phys. Rev. E. **73**, 031908, (2006)
 - [19] T. Aoyagi, Phys. Rev. Lett. **74**, 4075, (1995)
 - [20] J.Ch. Sturm, Bull. de Frussac , 11 (1829)
 - [21] L. S. Tsimring, A. Pikovsky, PRL **87** 250602 (2001)
 - [22] G . Le Masson, S. Renaud-Le Masson, D. Debay, T. Debay, Nature (London) **417**, 854, (2004)
 - [23] L.M. Pecora, T.L. Carroll, PRL **80**, 2109 (1998)
 - [24] T. Bal, D. Debay, A. Destexhe, Journal of Neuroscience, **20**, 7478, (2000)
 - [25] S. M. Sherman, R. W. Guillery, Exploring the Thalamus, Academic Press (Burlington) (2001)
 - [26] A. Destexhe, D. Contreras, M. Steriade, Journal of Neurophysiology, **79**, 999, (1998)